Mirror modes observed with Cluster in the Earth's magnetosheath : statistical study and IMF/solar wind dependence

V. Génot*, E. Budnik, C. Jacquey, I. Dandouras

CESR-CNRS-UPS, Observatoire Midi-Pyrénées, Toulouse, France,
**E-mail: vincent.genot@cesr.fr*

E. Lucek

The Blackett Laboratory, Imperial College, London, UK

We present a statistical analysis of 5 years of Cluster mission data in the magnetosheath. Our primary focus is to exhibit the spatial distribution of mirror mode events. The automatized detection is based on Minimum Variance Analysis and the amplitude of events. The results are displayed in the GIPM reference frame to enable comparison with a previous similar study using ISEE-1 data. These results compare favorably with each other and with studies focusing on Jupiter's and Saturn's magnetosheaths. We further analyze the dependence of the mirror events with solar wind parameters and Interplanetary Magnetic Field (IMF) orientation. We notably reveal that the occurrence of mirror modes is relatively more probable during periods of time when the IMF is not following the common Parker spiral orientation.

Keywords: Magnetosheath turbulence; Mirror mode; Statistical data analysis; Cluster observations

1. Introduction

Mirror mode structures in space plasma continue to fuel many new works in spite of an already vast literature on the subject. Hereafter some of the main characteristics of the mirror mode are reviewed to explained this abundant and active research activity. Its ubiquitousness : in environments of the Earth,[1,2] Jupiter,[4–6] Saturn,[7] Io wake,[8] the comet Halley,[9] solar wind,[10] ICME,[11] in the heliosheath[13,14] and even in turbulent galaxy clusters;[15] its peculiarity : a non-propagating mode, it is known as a fluid mode, obtained as one of the modes of anisotropic MHD, although it requires a kinetic

treatment (including Landau damping, see also Ref. 16) to properly determine the growth rate and because its transverse length scale extends to the order of the proton Larmor radius (see the discussion in Ref. 17); its potential existence at large to small length scales;[18] its role in plasma transport in particular near the magnetopause;[19] all of these features make of the mirror mode and mirror instability fundamental objects of study in plasma physics.

The threshold required for mirror instability to develop in a plasma is given by[20,21]

$$\beta_{p\perp}\left(\frac{T_{p\perp}}{T_{p\parallel}}-1\right)+\beta_{e\perp}\left(\frac{T_{e\perp}}{T_{e\parallel}}-1\right)>1+\frac{\left(\frac{T_{p\perp}}{T_{p\parallel}}-\frac{T_{e\perp}}{T_{e\parallel}}\right)^2}{2\left(\frac{1}{\beta_{p\parallel}}+\frac{1}{\beta_{e\parallel}}\right)} \tag{1}$$

where T is the temperature, $\beta = 2\mu_0 nkT/B^2$, subscripts $\perp$ and $\parallel$ stand for the directions with respect to the ambient magnetic field B, subscripts e and p are for electrons and protons respectively. For isotropic cold electrons this condition reduces to

$$\beta_{p\perp}\left(\frac{T_{p\perp}}{T_{p\parallel}}-1\right)>1 \tag{2}$$

Close to the Earth the best location for this condition to be met is in the magnetosheath (the temperature anisotropy and β values are indeed relatively large). Any observational study related to the mirror mode thus required a proper definition of the boundaries of the magnetosheath, the bow shock and the magnetopause, as well as a proper way of localization in this region. Long term operating missions such as ISEE and now Cluster enable the possibility of comprehensive statistical studies to reveal key dependence in the occurrence of wave modes with local and remotely controlling parameters. This is the main task of the present paper which addresses the occurrence and dependence issues of the mirror mode in the present Cluster context (see also Ref. 1,22). The paper is organized as follows. Section 2 presents the data and the way magnetosheath is identified. In section 3 the characterizing methods we employ for mirror modes are discussed. Section 4 exposes results of the statistical analysis with Cluster compared with results obtained from 10 years of ISEE-1 data,[2,3] whereas section 5 is concerned with solar wind and IMF dependencies. A summary of the main findings of the study concludes the paper in section 6.

2. Data

Five years of the Cluster mission are considered (01/02/2001 to 31/12/2005). Cluster 1 magnetic field (FGM[23]) and on-board calculated ion moments (from the HIA experiment on the CIS instrument[24]) data are used at 4 second resolution. We also employ ACE plasma and IMF data to determine the magnetopause and bow shock positions using models (as described below).

A web-based version of the statistical analysis tool developed at CDPP (the French Plasma Physics Data Centre) and used in this study is available at the URL : cdpp-amda.cesr.fr . Access is granted upon request (mail to amda@cesr.fr).

2.1. *Magnetosheath identification*

The first step of our analysis is to determine whether Cluster is located in the magnetosheath. Data are analyzed by 5min window : an iterative delay procedure is applied to obtain associated solar wind and IMF parameters from ACE. Bow shock[3] and magnetopause[25] models are computed from these parameters and Cluster is then identified as 'in' or 'out' the magnetosheath. Data will be displayed in the GIPM (geocentric interplanetary medium) reference frame first introduced by Ref. 46 and detailed in Ref. 3. This will enable consistent comparison with ISEE-1 results which are displayed in this frame in Ref. 3. For the sake of clarity we reproduce here the definition of this reference frame.

The X-axis $\vec{e_x}$ is antiparallel to the upstream solar wind velocity vector $\vec{V}$ in the reference frame moving with the planet (with components V_x, V_y, V_z in the GSE reference frame); the direction of the GIPM Y-axis is determined by the IMF vector $\vec{B}$ (with components B_x, B_y, B_z in the GSE reference frame):

$$\vec{e_y} = sgn(\vec{B}.\vec{e_x}).(-\vec{B} + (\vec{B}.\vec{e_x})\vec{e_x})/|\vec{B} - (\vec{B}.\vec{e_x})\vec{e_x}| \quad (3)$$

With such a definition an IMF field line lies in the second and fourth quadrants of the GIPM XY plane. Zenith angle (θ) and clock angle (ϕ) are defined by :

$$\theta = \arccos(\vec{r}.\vec{e_x}/r) \quad (4)$$

$$\phi = \arctan(\vec{r}.\vec{e_z}/\vec{r}.\vec{e_y}) \quad (5)$$

where $\vec{r}$ is a vector in the GSE frame. The clock angle is measured perpendicular to the solar wind direction. For an average IMF direction (following the Parker spiral) $-90° < \phi < 90°$ corresponds to the dusk magnetosheath side and $90° < \phi < 270°$ is on the dawn side.

In the following, we define our GIPM reference frame by using a 20min averaged (and shifted) IMF vector centred on the selected magnetosheath event.

2.2. *Fractional distance in the magnetosheath*

We will also make use of the fractional distance F introduced by Ref. 3 to normalize event positions in the magnetosheath :

$$F = \frac{r - r_{MP}}{r_{BS} - r_{MP}} \tag{6}$$

where r is the Cluster geocentric distance, r_{MP} is the geocentric distance to the magnetopause (which is a function of the zenith angle, the solar wind ram pressure and IMF B_z) and r_{BS} is the geocentric distance to the bow shock (which is a function of the zenith and clock angles, the upstream Alfvén and Mach numbers and the angle between the solar wind velocity and IMF vectors). Therefore $F = 0$ at the magnetopause and $F = 1$ at the bow shock.

3. Mirror mode characterization

Identification of mirror mode events has been a long standing problem because : 1/ slow mode and mirror mode have both anti-correlated magnetic and density fluctuations, 2/ mirror mode and ion cyclotron mode both grow on temperature anisotropy ($T_\perp > T_\parallel$). However in the magnetosheath it has been shown[26] and observed[27] that due to the presence of heavier ions (mainly helium) mirror instability dominates for $\beta > 1$ which is the most common situation, a condition confirmed by recent simulations[28] ($\beta_\parallel \geq 0.35$).

Along time, and with improving tools at hand, different methods have been developed to discriminate low frequency modes and among them the mirror mode. These include 1/ transport ratio,[29,30] 2/ minimum variance analysis,[2] 3/ 2- and 4- spacecraft methods,[16,31–33] 4/ 90° degree B/V_z phase difference.[34] A complete review is out of the scope of this article but the interested reader may refer to Ref. 35 for more details.

Multi-spacecraft studies have shown that mirror mode structures are elongated along a direction making a small angle with the ambient magnetic field.[1,33,36]

3.1. *Identification of mirror-like structures*

The magnetic field variations associated with mirror modes are almost linearly polarized parallel to the main field direction. They may be of large amplitude (a few 10%) of sinusoidal but also spiky up and down shapes as we shall discuss in section 4.4. From these characteristics, a criterion has been established which follows closely those used by Ref. 2,37 :

- linear polarization with field variation oriented close to the ambient magnetic field : the angle between the maximum variance direction and mean magnetic field vector is smaller than 20°.
- relatively large amplitude : the variance of the field is larger than 10%.

In order to perform statistical survey over 5 years of data we had to employ relatively low resolution data (4 s) which limits the lower sampled mirror event size to 8 s. From a 2 month survey with high resolution Cluster data, Ref. 37 found that mirror events were distributed as a bell shaped distribution with 98% of events falling into the 4s-24s interval and with a mean of 12 s. This shows that our data set is undersampled as it misses events in the 4 to 8s length which corresponds to the events with the smaller spatial scale (of the order of 10 local Larmor radius). However short duration mirror event does not automatically translate to short length scale event as the spacecraft velocity and geometry effects have to be taken into account. Therefore the undersampling of our dataset is not one-to-one equivalent to a bias toward large length scale mirror events. Nevertheless the way event scales are affecting statistics still remains to be studied with high resolution data.

The above criterion is applied to all 5min magnetosheath intervals obtained in the first step. The mean magnetic field is calculated on 10min window and the Minimum Variance Analysis[38] (MVA) and variance are performed on 5min windows. The sensitivity of the results has been tested against the variation of these time windows and revealed no major difference. At this stage we do not make any restriction on plasma parameter values as we are interested in mirror-like structures appearing above as well as below the linear mirror instability threshold given by Equation 2. No constraint has been imposed on the eigenvalues λ resulting from the MVA.

Indeed, as noted by Ref. 16 (from a small set of mirror events tough), mirror modes are more commonly observed as elliptically than linearly polarized as predicted by linear theory. It has been checked that restraining our data set to linear events (for instance with the condition : $\lambda_{int}/\lambda_{max} \leq 0.2$ and $\lambda_{min}/\lambda_{int} \geq 0.3$) does not significantly alter the conclusions drawn in the rest of the paper.

Let us note that Ref. 2 supplement their criterion with a condition on the symmetry of the structures which essentially selects magnetic depressions. Therefore 'dip' or 'hole' mirror modes only are discussed in that paper. This makes a significant difference between ISEE-1 and Cluster datasets which is discussed at the end of section 4.

Automatic detection of data patterns is hard to be perfect and it is therefore possible that compressional structures (like quasi-perpendicular shocks) other than mirror modes may be selected by our algorithm. It is however difficult to evaluate the proportion of misinterpreted events. In order to limit this occurrence we shall use error bars or plot data with only sufficient statistical significance.

3.2. *Mirror condition*

In order to qualify the plasma state with respect to the mirror instability we define the distance to threshold by

$$C_M = \beta_{p\perp} \left(\frac{T_{p\perp}}{T_{p\parallel}} - 1 \right) \tag{7}$$

From Equation 2, $C_M < 1$ ($C_M > 1$) corresponds to mirror (un)stable plasma while $C_M = 1$ denotes marginal stability for which the mirror growth rate is zero.

4. Cluster statistics and comparison with ISEE-1 data

Table 1. Ranges of parameters relative to the ISEE-1 mission[2,3] and Cluster mission (this study).

Mission	ISEE-1	Cluster
Time range	10 y	5 y
Time resolution	4 s	4 s
Fractional distance (F) range	0-1	0-1
Zenith angle (θ) range	$20° - 100°$	$0° - 150°$

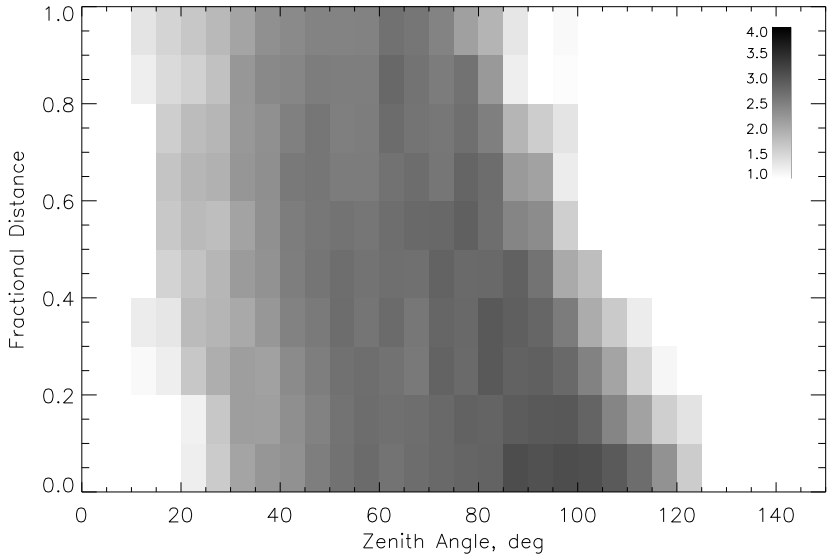

Fig. 1. Total number of magnetosheath crossings in the (zenith angle, fractional distance) plane. The grey scale is logarithmic.

The comparison exposed in this section is based on the results obtained by the algorithm presented in Section 3. Table 1 lists the range of orbital parameters associated with ISEE-1 and Cluster missions. Time resolutions of both these missions are identical.

On Figure 1 the total number of 5min magnetosheath crossings is displayed in the zenith angle - fractional distance plane in bins $\Delta\theta \times \Delta F = 5^\circ \times 0.05$. Events are integrated over all ϕ angles. The maximum number of crossings per bin is close to 10000. Cluster orbital configuration leads to a larger coverage close to the magnetopause and for high latitudes. In comparison ISEE-1 orbits covered a slightly reduced zenith angle range (see Table 1). Plotting data in a different plane, namely the clock angle - fractional distance plane (in bins $\Delta\phi \times \Delta F = 5^\circ \times 0.1$ integrated over $0^\circ \leq \theta \leq 150^\circ$, Figure not shown) illustrates that all regions of the magnetosheath are correctly sampled with a majority of events close to the magnetopause.

4.1. *Occurrence frequency*

The distribution of mirror mode events (ie 5min intervals which satisfy criteria of section 3.1) is displayed on Figure 2 (zenith angle - fractional distance plane) and Figure 3 (clock angle - fractional distance plane); bins with less than five magnetosheath crossings have been rejected in order to perform a statistically meaningful normalization. For this latter representation let us note that data from dawn (dusk) side of the magnetosheath are displayed on the left (right) part of the plot. Equivalently this corresponds to the quasi-parallel shock (quasi-perpendicular) region (see section 2.1 and Ref. 3 for more details on the GIPM reference frame). The number of events is divided by the total number of magnetosheath crossings to reveal the relative number of mirror events (or occurrence frequency). This shows that mirror events are more likely to occur close to the magnetopause for all zenith angles and for smaller and smaller angles for increasing distance from the magnetopause. The dark bin at $(\theta = 112.5°, F = 0.35)$ is a statistical artefact. There is a dawn/dusk asymmetry with more events occurring in the dusk sector which is also the region connected to quasi-perpendicular shock after which mirror modes are mostly expected. Indeed larger temperature anisotropies are generally encountered behind perpendicular shocks rather than parallel ones due to a sharper transition from solar wind to magnetosheath plasmas (see also the theoretical work in Ref. 12). These results agree with those of Ref. 2 and Ref. 3. Although our data representation is more pixelized than in Ref. 3, occurrence frequencies cannot be one to one compared as normalization has been applied differently. The present findings are also consistent with observations from Equator-S data which show that mirror modes are mostly encountered in the inner magnetosheath region.[39]

4.2. *Amplitude distribution*

The amplitude distribution of mirror mode events $\delta B/B$ is displayed on Figure 4 in a representation equivalent to Figure 3; bins with less than five mirrors events have been rejected in order for the statistics to be meaningful. There is a tendency to observe larger events in the middle magnetosheath although the distribution is scarce close to the shock. Also the average intensity of mirror structures is generally larger in the morning magnetosheath ($90° < \phi < 270°$) compared to the evening magnetosheath region ($-90° < \phi < 90°$). It is more precisely in the pre-dawn quadrant that mirror amplitudes are the larger ($90° \leq \phi \leq 135°$) in close agreement

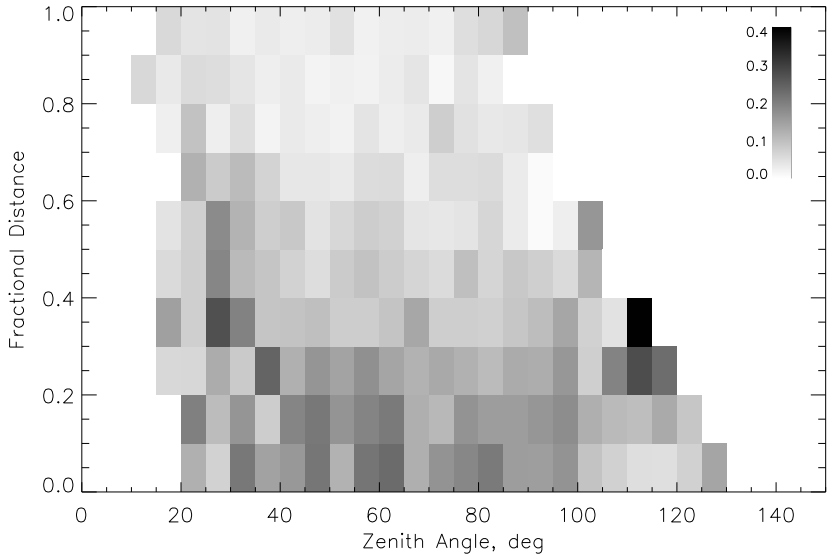

Fig. 2. Relative number of mirror mode events in the (zenith angle, fractional distance) plane. The grey scale codes the occurrence frequency and bins with less than five magnetosheath crossings have been rejected.

with ISEE-1 results.

Ref. 3 argues that there may be a bias effect due the high level of turbulence behind the parallel bow shock which hides low amplitude mirror fluctuations. A similar effect may affect our data or, if this is a real physical feature, the process behind it remains not fully understood.

The results from Cluster observations are however consistent with those obtained from ISEE-1 reported in Ref. 2 and Ref. 3 : the maximum value for $\delta B/B$ is comparable ($\sim$0.5 in both studies). They also compare favorably with results from studies on giant planets. At Saturn, Ref. 7 found that the amplitude and wavelength of fluctuations tend to increase with increasing distance from the quasi-perpendicular bow shock, except close to the magnetopause in the plasma depletion layer. At Jupiter, Ref. 4 studied the statistical properties of mirror mode depressions observed by Ulysses and found that the amplitude of the fluctuations was decreasing when approaching the bow shock. Naturally mirror waves need time to grow from their supposed origin at the shock, and as simultaneously they are convected towards the planet, larger fluctuations are seen away from the shock. Close to

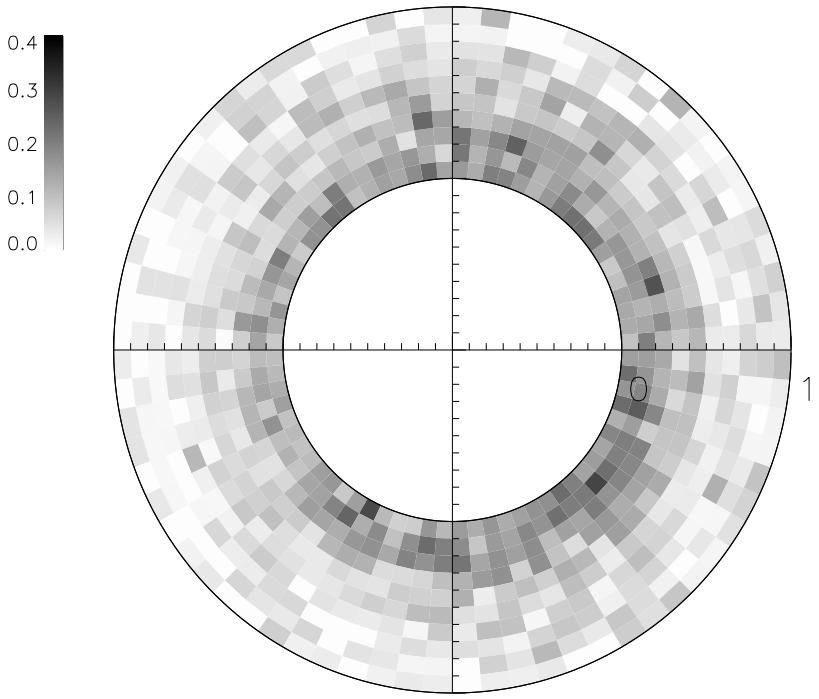

Fig. 3. Relative number of mirror mode events in the (clock angle, fractional distance) plane. The grey scale codes the occurrence frequency and bins with less than five magnetosheath crossings have been rejected.

the magnetopause 1/ the free energy contained in the anisotropy may have been consumed by instabilities, 2/ the wave growth may have saturated or 3/ the plasma flow has been deviated (near the plasma depletion layer) which explained why amplitude does not peak close to the magnetopause.

4.3. *Growth rate*

Following Ref. 40, Ref. 11 derived an expression for the maximum growth rate of the mirror instability (normalized to the proton cyclotron frequency Ω_p) :

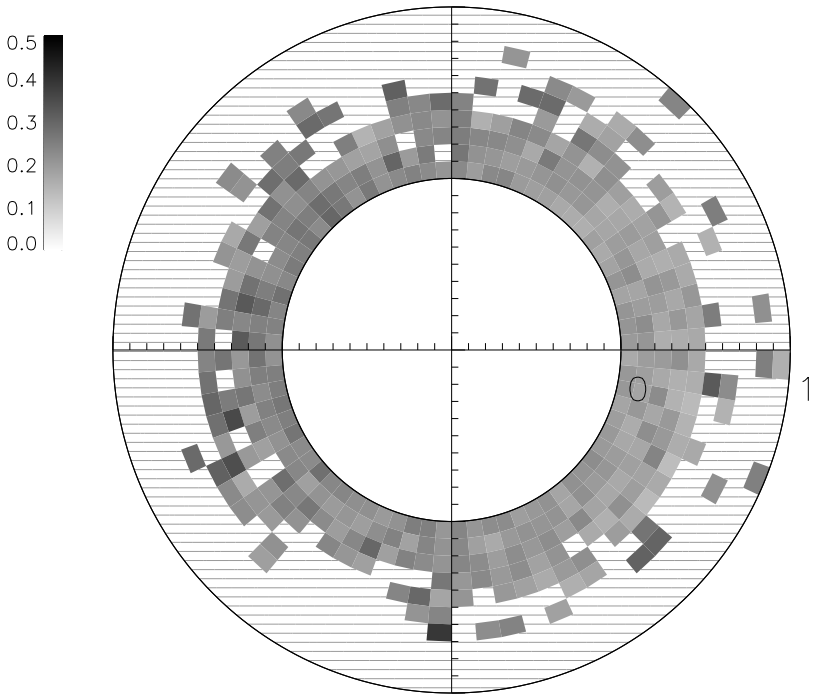

Fig. 4. Relative mirror mode amplitude ($\delta B/B$) in the (clock angle, fractional distance) plane. The grey scale codes the magnitude of the magnetic field perturbation and bins with less than five mirrors events have been rejected.

$$\frac{\gamma_m}{\Omega_p} = \frac{1}{\sqrt{12\pi}\beta_\perp}\left(\frac{T_{p\perp}}{T_{p\|}}\right)^{-3/2}\left(\beta_\perp\left(\frac{T_{p\perp}}{T_{p\|}}-1\right)-1\right)^2 \tag{8}$$

for the conditions $k_\| \ll k_\perp$ in the long wavelength limit and $C_M > 1$ (see Equation 7).

Based on a numerical evaluation of the full kinetic dispersion relation, this maximum growth rate is $\gamma_m/\Omega_p \simeq 0.02$ for a plasma containing $5-10\%$ alpha particles, $T_\perp/T_\| = 1.5$, $T_{\alpha\|} = 4T_{p\|}$, and $\beta_\perp$=4 (see Ref. 26 and Ref. 47). With these plasma parameters the above equation also yields

$\gamma_m/\Omega_p \simeq 0.02$. Let us note that since this value is significantly larger than the maximum growth rate of the proton cyclotron instability, mirror waves can grow faster.

By using Equation 8, therefore selecting mirror events with $C_M > 1$ only in our analysis, maximum growth rate is evaluated to be below the $\gamma_m/\Omega_p = 0.1$ level whereas 77% of events are below the $\gamma_m/\Omega_p = 0.01$ level; the mean value is 0.008. These values are consistent with observations and simulations showing that the magnetosheath plasma is mostly in a marginal state with respect to the mirror instability.[28]

Using a model of plasma flowlines and data from the ISEE-1 spacecraft, Ref. 41 showed that the growth rate values are in the range 0.002 $s^{-1} < \gamma <$0.0035 s^{-1}, which is almost an order of magnitude smaller than the value calculated by Ref. 26. These growth rate are not maximum values but are computed from the evolution of $\delta B/B$ along flow lines. Ref. 41 propose several reasons for this discrepancy one of which being that the source of the mirror fluctuations may not be at the bow shock but at various locations more deep inside the magnetosheath. Also the linear analysis done by Ref. 26 might not be applicable to large amplitude nonlinear fluctuations. However we note that the authors restrained their dataset to magnetic dips (or holes) only. Recent works[17,43] have shown that such magnetic configurations generally 1/ correspond to a late evolutionary stage of mirror modes (nonlinear regime) and 2/ are observed in mirror stable plasma ($C_M < 1$), both conditions in which application of Equation 8 or linear theory is not appropriate.

4.4. *Discussion : differences between ISEE-1 and Cluster datasets*

As discussed above the algorithm in Ref. 2 retained only magnetic depressions whereas our present results concern all magnetic shapes. This is not an innocuous remark. Indeed the shape of mirror modes had recently attracted attention both from the theoretical[17,42] and observational[6,37,43] points of view. These works gave new insight in the physics governing the evolution of the mirror instability. Previous studies had identified that mirror structures came in different shapes,[16,39] but it is only recently that it was revealed that the shape was controlled by the distance to the threshold C_M. It was concluded that deep holes are mainly due to a bistability process (enabling the existence of mirror structures in mirror stable plasma conditions, $C_M < 1$), moderate holes and peaks may be observed near threshold, and large peaks are non linearly saturated mirror mode struc-

tures far from threshold. The localization of these different structures in the magnetosheath showed that holes are preferentially observed close to the magnetopause whereas peaks are more frequent in the middle magnetosheath. This spatial distribution is illustrated on Figure 5 which shows the value of C_M in the (zenith angle, fractional distance) plane : maximum value, corresponding to peaks, are obtained in the middle magnetosheath whereas close to the magnetopause C_M is close or less than one denoting the presence of holes. The proportion of events with $C_M > 1$ ($C_M < 1$) is 50% (50%). A more detailed description is out of the scope of the present paper (the relation shape/C_M is exposed extensively in Ref. 37,43) but these remarks enable to pinpoint differences between our present analysis and the one based on ISEE-1. Ref. 2 retained magnetic depressions only, mostly observed in mirror stable plasmas close to the magnetopause, whereas our analysis is more general in keeping all mirror-like structures without constraining plasma parameters. However observations show that peaks are a minority (14% of events in Ref. 6, 18.7% in Ref. 37 for 19% and 39.7% of hole structures respectively) in mirror datasets; simulations also show that large mirror peaks only survive in seldom encountered large β plasmas.[43] This may explain why results compare favorably between both studies despite differences in initial datasets.

5. Relation with solar wind parameters and IMF orientation

Table 2. Mean values of solar wind and IMF parameters for mirror and non-mirror types of events.

Type of event	mirror	non-mirror
Number of events	6363	57405
alpha/proton density ratio	0.0453	0.0448
ram pressure (nPa)	2.33	2.12
M_A ($M_A^2 = 4\pi\rho V^2/B^2$)	*10.91*	*8.17*
M_s ($M_s^2 = \rho V^2/\gamma p$)	8.68	8.49
γ_m/Ω_p	0.008	-

We use ACE data and a solar wind-magnetosheath iterative delay algorithm to associate each magnetosheath event to corresponding solar wind and IMF parameters. From the values given in Table 2 it is interesting to note that mean values for both kinds of events (mirror and non-mirror) are not significantly different, except for M_A. In this particular case, the striking difference led us to investigate this dependence into more details.

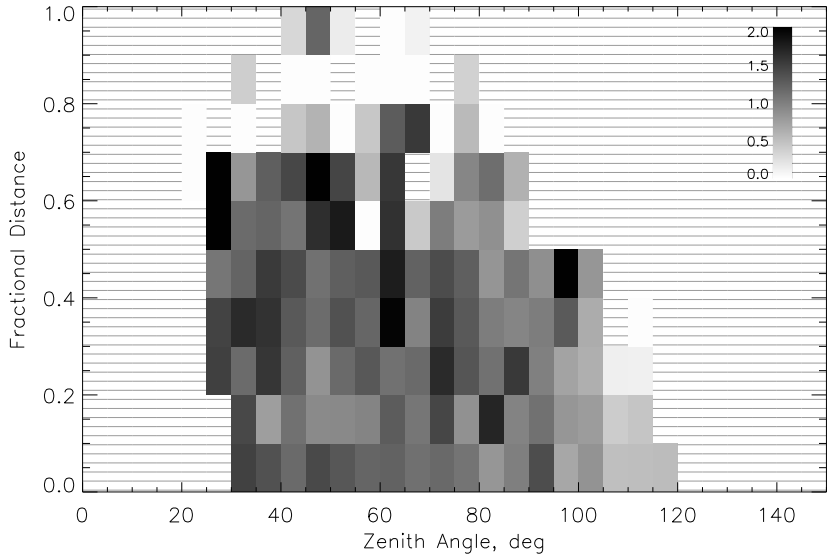

Fig. 5. Distribution of the average distance to threshold (C_M) of the events in the (zenith angle, fractional distance) plane.

5.1. M_A dependence

On Figure 6 the distribution of events with M_A bins (of width 1) is plotted : the dash line is for all magnetosheath 5min intervals whereas the solid line refers to identified mirror modes only, both normalized to their maximum value. Distributions exhibit clear peaks with a larger most probable value for mirror events ($\max(M_A = 8.5)$) than for non mirror associated traversals ($\max(M_A = 6.5)$). The average value of the distribution is also higher for mirror events (10.91 to be compared to 8.17, see Table 2). The ratio between these two distributions is plotted on Figure 7 to reveal that the occurrence frequency of mirror modes increases as a function of M_A until $M_A = 12$. This increasing trend is the prominent feature of the Figure as more than 80% of mirror events occur for $M_A \leq 12$.

As the distribution of mirror events with the ram pressure does not show significant shift compared with the distribution of magnetosheath crossings (and equivalently for the dependence with M_s; not shown, see mean values in Table 2), the dependence on M_A translates into a dependence on the IMF magnitude. Whereas the upstream (IMF) and downstream (magne-

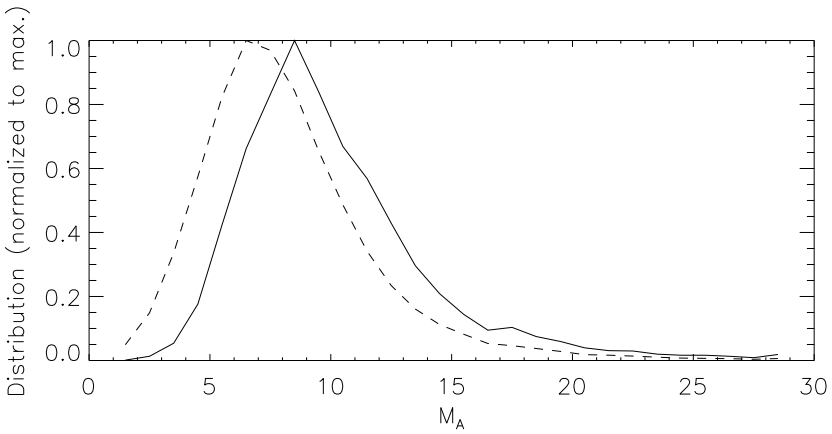

Fig. 6. Distributions of mirror-like structures (solid line) and of all magnetosheath crossings (dash line) as a function of M_A.

tosheath) magnetic fields are (positively) correlated it is less clear for the temperature. Therefore, as mirror modes are favoured by large β ($\propto 1/B^2$) conditions, this magnetic field correlation can tentatively explain the variation with M_A ($\propto 1/B$).

As solar wind perturbations acting on the global response of the magnetosphere is studied to exhibit geo-effectiveness, the solar wind parameters acting decisively on the growth of mirror modes has to be studied into more details, and this beyond the 'simple' filtering effect of the bow shock which has evidently to be taken into account, as we discuss below.

5.2. *IMF orientation*

The occurrence of mirror mode signatures in relation with the IMF orientation has been analyzed. Mirror mode are usually more frequently observed behind quasi-perpendicular shocks (see Section 4.1), which for common orientation of the IMF (along the Parker spiral) corresponds to dusk side. To construct Figure 8, for each 5min magnetosheath crossing, we recorded the associated IMF orientation and plotted the corresponding point in the (B_x, B_y) plane (in GSE coordinates). In this plane most of the points are observed in the second and fourth quadrants along the $B_y = -B_x$ line which correspond to the 45 degrees Parker spiral (proportions of events in quadrants $2-4$ and $1-3$ are 77% and 23% respectively). When we retain mirror mode events only the picture is changed as the other two quadrants

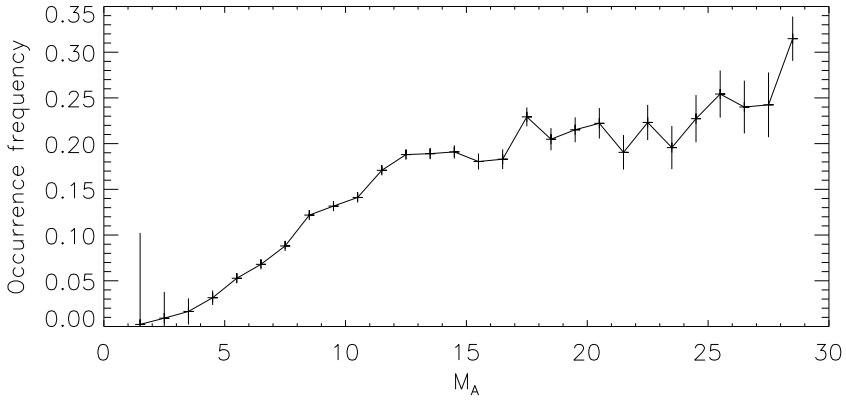

Fig. 7. Occurrence frequency of mirror-like structures as a function of M_A. The error bars are proportional to $1/\sqrt{N}$ where N is the number of mirror events in each $\Delta M_A = 1$ bin ($N_{min} = 1$ and $N_{max} = 909$).

exhibit significantly more points, making the distribution appear like a ring (proportions are then 70%/30%). When one plots the relative number of events (Figure 9) the result is even more striking as it appears clearly that this relative number is higher for IMF direction perpendicular to the average Parker spiral. This original result has also been observed with ISEE data (M. Tátrallyay, private communication). Indeed ISEE data revealed that there were relatively more events at the time of non-typical IMF directions compared to the events when the IMF was closer to the Parker spiral direction : in about 75% of all observations the IMF was in the Parker quadrants, whereas for about 25% of all observations the IMF was in the non-typical quadrants; but only about 70% of the selected mirror events were in the Parker quadrants, and about 30% of these events were in the non-typical quadrants. These values are remarkably consistent with those obtained with Cluster data. Therefore, according to these numbers the selected mirror events occurred more than 30% more frequently when the IMF is not in the Parker spiral direction (ie an increase from 23% to 30% in the Cluster case).

Similar plots with Cluster data in the (B_y, B_z) plane (not shown) exhibit a smaller increase of this occurrence frequency for non-Parker situations ($\sim$7% to be compared to the 30% above).

To understand fully the process behind this counter-intuitive observa-

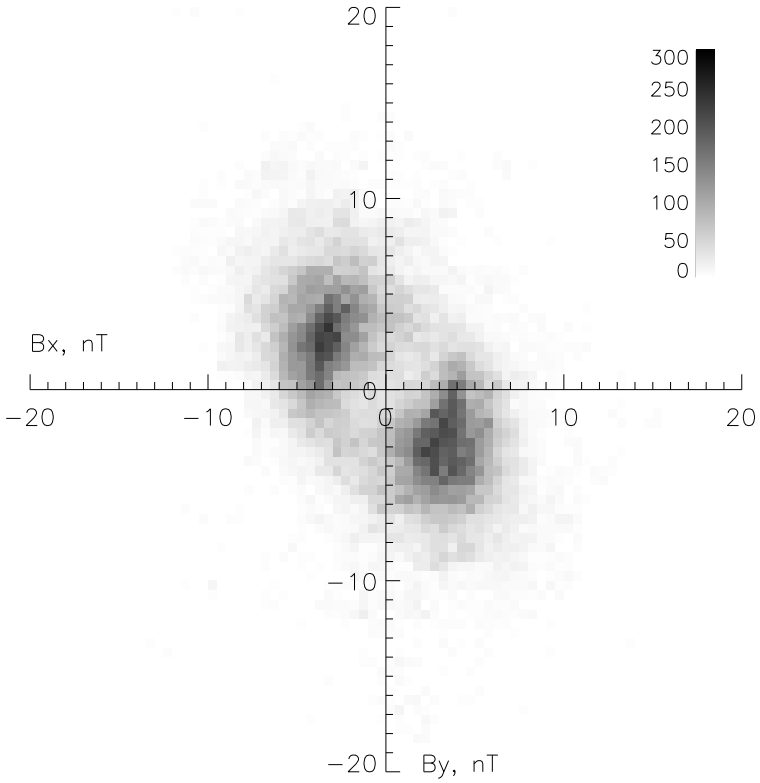

Fig. 8. IMF in the XY_{GSE} plane for all magnetosheath crossings. The grey scale codes the number of events in each 0.5nT×0.5nT bin.

tion one needs to compute correctly the nature of the shock associated with each mirror events. This implies using a streamline model (derived from Ref. 44 for instance) or simulation results (like it is done in Ref. 6 using a model by Ref. 45) which is left for future work.

6. Summary and conclusion

We have used 5 years of Cluster magnetosheath crossings to investigate the occurrence of fluctuations associated with the mirror instability. No constrain was imposed on the plasma parameters, as it is recognized that mirror

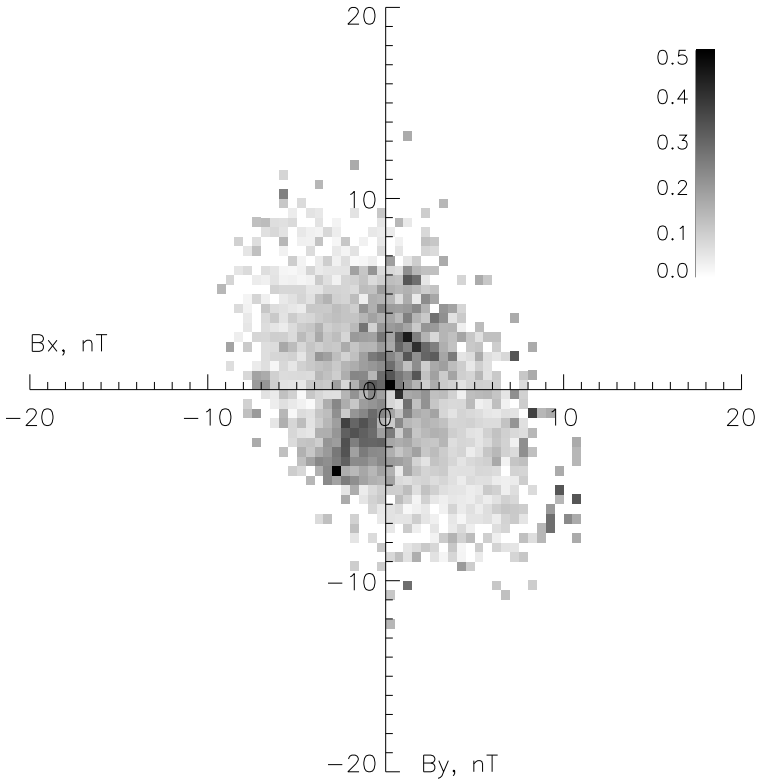

Fig. 9. IMF in the XY_{GSE} plane for mirror only events normalized to the total number of crossings. The grey scale codes the occurrence frequency and bins with less than five crossings have been rejected.

structures also exist below the mirror instability linear threshold (mainly in the form of magnetic holes[43]). Let us summarize the main findings of the paper.

- There is a larger occurrence in the inner region of the magnetosheath, close to the magnetopause at larger zenith angle and closer to the middle of the sheath in the subsolar region.
- There is a dawn/dusk asymmetry with more events occurring in the dusk sector, i.e. behind quasi-perpendicular shocks.

- Mirror fluctuation amplitudes are larger in the middle magnetosheath (despite a small statistical coverage close to the shock).
- There is a dawn/dusk asymmetry with more large amplitude events occurring in the dawn sector, i.e. behind quasi-parallel shocks.
- There is no significant dependence with M_s or with the ram pressure of the solar wind.
- There is a clear dependence with M_A which, given the above remarks, translates into a dependence with the IMF amplitude B.
- There is a clear dependence with the IMF $(B_x, B_y)_{GSE}$ angle with relatively more mirror events (+30%) occurring at times when the IMF is not oriented along the Parker spiral.

Such conclusions could be interesting for integration in further modeling efforts. Indeed clarifying the space of potentially influencing parameters is crucial for studying the evolution of the mirror instability. For instance it is such an observational study on mirror structures shapes which paved the way to identify the bistability phenomenon which is behind the shape/localization mirror structure filtering in the magnetosheath. Improvements in the present analysis could imply the use of a plasma flow line model to relate properly the events to their originating bow shock localization. Regarding the influence of the solar wind, this analysis clearly opened new questions (role of IMF magnitude and orientation) which demand a parametric study to be properly addressed using numerical simulations.

acknowledgements

This work was performed in the frame of the International Space Science Institute meetings of Team 80 "The effect of ULF turbulence and flow chaotisation on plasma energy and mass transfer at the magnetopause". We thank the CDPP team members for their efforts in developing the analysis tools used in this study. VG also thanks M. Tátrallyay, P. Hellinger, T. Passot, and G. Belmont for fruitful discussions.

References

1. Lucek, E. A., Dunlop, M. W., Horbury, T. S., Balogh, A., Brown, P., Cargill, P., Carr, C., Fornaçon, K.-H., Georgescu, E., and Oddy, T., Cluster magnetic field observations in the magnetosheath: four-point measurements of mirror structures, *Ann. Geophys., 19*, 10, 1421, 2001.
2. Tátrallyay, M., and G. Erdös, Statistical investigation of mirror type magnetic field depressions observed by ISEE-1, *Planet. Space Sci., 53,* 33, 2005.

3. Verigin, M.I., M. Tátrallyay, G. Erdös and G.A. Kotova, Magnetosheath-Interplanetary medium reference frame : Application for a statistical study of mirror type waves in the terrestrial plasma environment, *Adv. Space Res., 37,* 515, 2006.
4. Erdös, G., and A. Balogh, Statistical properties of mirror mode structures observed by Ulysses in the magnetosheath of Jupiter, *J. Geophys. Res., 101*, 112, 1996.
5. André N., G. Erdös, and M. Dougherty, Overview of mirror mode fluctuations in the jovian dusk magnetosheath: Cassini magnetometer observations, *Geophys. Res. Lett., 29* (20), 1980, doi:10.1029/2002GL015187, 2002.
6. Joy, S. P.; Kivelson, M. G.; Walker, R. J.; Khurana, K. K.; Russell, C. T.; Paterson, W. R., Mirror mode structures in the Jovian magnetosheath, *J. Geophys. Res., 111,* 2006.
7. Bavassano Cattaneo, M. B., C. Basile, G. Moreno, and J. D. Richardson, Evolution of mirror structures in the magnetosheath of Saturn from the bow shock to the magnetopause, *J. Geophys. Res., 103*, 11,96111,972, 1998.
8. Huddleston, D. E., R. J. Strangeway, X. Blanco-Cano, C. T. Russell, M. G. Kivelson, K. K. Khurana, Mirror-mode structures at the Galileo-Io flyby: Instability criterion and dispersion analysis, *J. Geophys. Res., 104* (A8), 17479-17490, 10.1029/1999JA900195, 1999.
9. Russell, C. T., Riedler, W., Schwingenschuh, K., and Yeroshenko, Y., Mirror instability in the magnetosphere of Comet Halley, *Geophys. Res. Lett.*, 14, 1987.
10. Winterhalter, D., M. Neugebauer, B. E. Goldstein, E. J. Smith, S. J. Bame, and A. Balogh, Ulysses field and plasma observations of magnetic holes in the solar wind and their relation to mirror-mode structures, *J. Geophys. Res., 99*, 23,37123,381, 1994.
11. Liu, Y.; Richardson, J. D.; Belcher, J. W.; Kasper, J. C.; Skoug, R. M., Plasma depletion and mirror waves ahead of interplanetary coronal mass ejections, *J. Geophys. Res., 111,* 2006.
12. Liu, Y., Richardson, J. D., Belcher, J. W., and Kasper, J. C., Temperature anisotropy in a shocked plasma: Mirror-mode instabilities in the heliosheath, *Astrophys. Journal, 659,* 2007.
13. Burlaga L. F., N. F. Ness, M. H. Acũna (2006), Trains of magnetic holes and magnetic humps in the heliosheath, *Geophys. Res. Lett., 33*, L21106, doi:10.1029/2006GL027276.
14. Burlaga L. F., N. F. Ness, M. H. Acuna (2007), Linear magnetic holes in a unipolar region of the heliosheath observed by Voyager 1, *J. Geophys. Res., 112, A07106*, doi:10.1029/2007JA012292.
15. Schekochihin, A. A., Cowley, S. C., Kulsrud, R. M., Rosin, M. S., and Heinemann, T., Nonlinear growth of firehose and mirror fluctuations in turbulent galaxy-cluster plasmas, *ArXiv e-prints*, 0709.3828, 2007.
16. Génot, V., S. J. Schwartz, C. Mazelle, M. Balikhin, M. Dunlop, T. M. Bauer, Kinetic study of the mirror mode, *J. Geophys. Res., 106(A10)*, 21611-21622, 10.1029/2000JA000457, 2001.
17. Passot T., V. Ruban, P. L. Sulem (2006), Fluid description of trains of stationary mirror structures in a magnetized plasma, *Phys. Plasmas, 13*, 102310.

18. Sahraoui F, Belmont G, Rezeau L, Cornilleau-Wehrlin N, Pincon JL, Balogh A, Anisotropic turbulent spectra in the terrestrial magnetosheath as seen by the cluster spacecraft, *Phys. Rev. Lett.,96(7)*, 075002, 2006.
19. Johnson, J. R., C. Z. Cheng, Global structure of mirror modes in the magnetosheath, J. Geophys. Res., 102(A4), 7179-7190, 10.1029/96JA03949, 1997.
20. Hall, A. N., *J. Plasma Phys., 21*, 431, 1979.
21. Hellinger P., Comment on the linear mirror instability near the threshold, *Phys. Plasmas, 14*, 8, 2007.
22. Constantinescu O. D., K.-H. Glassmeier, R. Treumann, K.-H. Fornacon, Magnetic mirror structures observed by Cluster in the magnetosheath, *Geophys. Res. Lett., 30 (15)*, 1802, doi:10.1029/2003GL017313, 2003.
23. Balogh, A., et al. The Cluster Magnetic Field Investigation: overview of in-flight performance and initial results, *Ann. Geophys.*, 19, 1207, 2001.
24. Rème, H. et al., First multispacecraft ion measurements in and near the Earth's magnetosphere with the identical Cluster ion spectrometry (CIS) experiment, *Ann. Geophys., 19*, 10, 1303-1354, 2001.
25. Shue, J.-H.; Chao, J. K.; Fu, H. C.; Russell, C. T.; Song, P.; Khurana, K. K.; and Singer, H. J., A new functional form to study the solar wind control of the magnetopause size and shape, *J. Geophys. Res., 102*, 5, 9497, 1997.
26. Gary, S. P., S. A. Fuselier, B. J. Anderson, Ion anisotropy instabilities in the magnetosheath, *J. Geophys. Res., 98(A2)*, 1481-1488, 10.1029/92JA01844, 1993.
27. Anderson, B. J., S. A. Fuselier, S. P. Gary, R. E. Denton, Magnetic spectral signatures in the Earths magnetosheath and plasma depletion layer, *J. Geophys. Res., 99(A4)*, 5877-5892, 10.1029/93JA02827, 1994.
28. Trávníček, P., Hellinger, P., Taylor, M. G. G. T., Escoubet, C. P., Dandouras, I. and Lucek, E., Magnetosheath plasma expansion : hybrid simulations, *Geophys. Res. Lett., 34 (15)*, doi:10.1029/2007GL029728, 2007.
29. Song, P., C. T. Russell, S. P. Gary, Identification of low-frequency fluctuations in the terrestrial magnetosheath, *J. Geophys. Res., 99(A4)*, 6011-6026, 10.1029/93JA03300, 1994.
30. Denton, R. E., S. P. Gary, B. J. Anderson, J. W. LaBelle, M. Lessard, Low-frequency fluctuations in the magnetosheath near the magnetopause, *J. Geophys. Res., 100(A4)*, 5665-5680, 10.1029/94JA03024, 1995.
31. Chisham, G., S. J. Schwartz, M. A. Balikhin, M. W. Dunlop, AMPTE observations of mirror mode waves in the magnetosheath: Wavevector determination, *J. Geophys. Res., 104(A1)*, 437-448, 10.1029/1998JA900044, 1999.
32. Balikhin M. A., O. A. Pokhotelov, S. N. Walker, E. Amata, M. Andre, M. Dunlop, H. S. C. K. Alleyne, Minimum variance free wave identification: Application to Cluster electric field data in the magnetosheath, *Geophys. Res. Lett., 30 (10)*, 1508, doi:10.1029/2003GL016918, 2003.
33. Horbury, T. S., E. A. Lucek, A. Balogh, I. Dandouras, and H. R'eme (2004), Motion and orientation of magnetic field dips and peaks in the terrestrial magnetosheath, *J. Geophys. Res., 109*, 9209, doi:10.1029/2003JA010237.
34. Lin, C.-H., J. K. Chao, L. C. Lee, D. J. Wu, Y. Li, B. H. Wu, P. Song, Identification of mirror waves by the phase difference between perturbed magnetic

field and plasmas, *J. Geophys. Res., 103(A4)*, 6621-6632, 10.1029/97JA03474, 1998.
35. Schwartz, S. J., D. Burgess, and J. J. Moses (1996), Lowfrequency waves in the Earths magnetosheath: present status, *Ann. Geophysicae, 14*, 11341150.
36. Fazakerley, A. N., and D. J. Southwood, Mirror instability in the magnetosheath, *Advances in Space Research, 14*, 7, 65, 1994.
37. Soucek, J., E. Lucek, and I. Dandouras, Properties of magnetosheath mirror modes observed by Cluster and their response to changes in plasma parameters, *J. Geophys. Res., in press.*
38. Sonnerup, B. U. O., and L. J. Cahill Jr., Magnetopause structure and attitude from Explorer 12 observations, *J. Geophys. Res., 72*, 171, 1967.
39. Lucek, E. A.; Dunlop, M. W.; Balogh, A.; Cargill, P.; Baumjohann, W.; Georgescu, E.; Haerendel, G.; Fornacon, K.-H., Identification of magnetosheath mirror modes in Equator-S magnetic field data, *Ann. Geophys., 17*, 12, 1999.
40. Hasegawa, A. (1969), Drift mirror instability in the magnetosphere, *Phys. Fluids*, 12, 2642.
41. Tatrallyay, M., and G. Erdös (2002), The evolution of mirror mode fluctuations in the terrestrial magnetosheath, *Planet. Space Sci.*, 50, 593599.
42. Kuznetsov, E. A., T. Passot, and P. L. Sulem (2007), Dynamical Model for Nonlinear Mirror Modes near Threshold, *Phys. Rev. Lett., 98*, 235,003.
43. Génot, V., E. Budnik, P. Hellinger, T. Passot, G. Belmont, P. Trávnícek, E. Lucek, and I. Dandouras, Mirror structures above and below the linear instability threshold : Cluster observations, fluid model and hybrid simulations, *submitted to Annales Geophysicae*, 2008.
44. Spreiter J.R. and Stahara S.S. (1980) A new predictive model for determining solar wind - terrestrial planet interactions. *J. Geophys. Res.*, 85, 6769
45. Ogino, T., R. J. Walker, and M. G. Kivelson (1998), A global magnetohydrodynamic simulation of the Jovian magnetosphere, *J. Geophys. Res.*, 103, 225.
46. Bieber and Stone, 1979 Bieber, J.W., Stone, E.C. Energetic electron bursts in the magnetopause electron layer and in interplanetary space, in: Proceedings of Magnetospheric Boundary Layers Conference, Alpbach, 1115 June 1979, ESA SP-148, pp. 131135, 1979.
47. Hubert, D., Lacombe, C., Harvey, C.C., Moncuquet, M., Nature, properties, and origin of low-frequency waves from an oblique shock to the inner magnetosheath, *J. Geophys. Res., 103*, 26783, 1998.